Dairy Sci. Technol. 89 (2009) 301–316
© INRA, EDP Sciences, 2009
DOI: 10.1051/dst/2009019

Available online at:
www.dairy-journal.org

Original article

Effects of pH and Ca/P molar ratio on the quantity and crystalline structure of calcium phosphates obtained from aqueous solutions

Omar Mekmene[1,2], Sophie Quillard[2], Thierry Rouillon[2], Jean-Michel Bouler[2], Michel Piot[1], Frédéric Gaucheron[1*]

[1] INRA, UMR1253 Science et Technologie du Lait et de l'Œuf, 65 rue de Saint Brieuc, 35042 Rennes Cedex, France
[2] INSERM, U791 Laboratoire d'Ingénierie Ostéo-Articulaire et Dentaire, Faculté de chirurgie dentaire, Université de Nantes, 1 place Alexis Ricordeau, 44042 Nantes, France

Received 12 November 2008 – Accepted 16 April 2009

Abstract – Milk and dairy products contain large amounts of calcium phosphate salts that can precipitate. The chemical composition and the crystalline structure of the calcium phosphate precipitates that are formed in dairy industry depend on the physico-chemical conditions, particularly, pH and mineral composition. The objective of this study was to determine, using mineral solutions, the effects of pH and of the concentrations of calcium and phosphate on the quantity and crystalline structure of calcium phosphate precipitates. Experiments were carried out at 20 °C with 20.00 mmol·L^{-1} phosphate and three Ca/P molar ratios (1.00, 1.50 and 2.00). The initial pH (5.50, 6.70, 7.50, 8.50 and 9.50) were drifting or kept constant during a reaction time of 3 h. After filtration of the suspensions, the mineral compositions of filtrates were quantified. The lyophilized precipitates were characterized using X-ray diffraction, infrared spectroscopy and scanning electron microscopy techniques. At drifting pH (final pH values were between 4.6 and 6.0), the mineral analyses showed that the Ca/P ratio did not influence the amounts of precipitated calcium and phosphate. The analyses of precipitates revealed the formation of brushite as the main crystalline phase. At constant pH, the mineral analyses showed that the Ca/P ratio strongly influenced the precipitation efficiency of calcium phosphate. The analyses of precipitates revealed the formation of poorly crystallized calcium-deficient apatites. A decrease of crystallinity with an increase in initial pH was observed. In conclusion, pH can be a key factor to control the quantity and crystalline structure of calcium phosphates obtained by precipitation. This factor should be considered for the recovery of calcium phosphates from dairy co-products. pH is also important in the fouling phenomena of membranes and heat exchangers caused by calcium phosphate precipitation.

milk / dairy product / calcium phosphate / precipitation / brushite

摘要 – pH 和 Ca/P 摩尔比对磷酸钙的产量和晶体结构的影响。乳和乳制品中含有丰富的、可沉淀的磷酸钙。从乳制品中获得磷酸钙沉淀的化学组成和晶体结构完全决定于发生反应的物理和化学条件，特别是 pH 和矿物元素的组成。通过调整 pH、钙浓度和磷酸盐浓度，研究这些因素对生成磷酸钙沉淀的产量和晶体结构的影响。在 20 °C 下，20.00 mmol·L^{-1} 的磷酸盐和 3 组不同 Ca/P 摩尔比的溶液（1.00、1.50、2.00）发生反应，初始 pH（5.50、6.70、

*Corresponding author (通讯作者): frederic.gaucheron@rennes.inra.fr

7.50、8.50、9.50）是变化或者保持不变，整个反应时间为 3 小时。悬浮液过滤，准确称量沉淀物。冻干的沉淀物经 X-射线衍射、红外光谱和扫描电镜技术表征。在变化的 pH 下（最终的 pH 是在 4.6 和 6.0），根据对矿物元素的分析表明 Ca/P 摩尔对磷酸钙的沉淀量没有影响；而对沉淀物的分析则显示在主要的晶相中存在透钙磷石（$CaHPO_4{\cdot}2H_2O_2$）。在保持恒定 pH 条件下，矿物元素的分析结果表明 Ca/P 摩尔比对磷酸钙的沉淀效率有显著的影响，而对磷酸钙的沉淀物分析则显示由于形成聊不完全的磷灰石使得钙盐晶体非常差。随着初始 pH 的增加结晶度降低。因此，对沉淀法生产磷酸钙沉淀而言，pH 是控制产量和晶体结构的主要因素。这种方法可以用来从乳品工业的共产物中回收磷酸钙。同时由于 pH 变化导致的磷酸钙沉淀也是造成膜和热交换器堵塞得重要原因。

乳 / 乳制品 / 磷酸钙 / 沉淀 / 透钙磷石

Résumé – Effets du pH et du ratio molaire Ca/P sur la quantité et la structure cristalline des phosphates de calcium obtenus à partir de solutions aqueuses. Le lait et les produits laitiers sont riches en sels de phosphate de calcium qui peuvent précipiter. La composition chimique et la structure cristalline de ces précipités formés en industrie laitière dépendent des conditions physicochimiques de formation, notamment le pH et la composition minérale. L'objectif de ce travail était de déterminer, en utilisant des solutions minérales, les rôles du pH et des concentrations du calcium et du phosphate sur la nature et la quantité des précipités de phosphate de calcium. Les expériences ont été réalisées à 20 °C, avec une concentration en phosphate de 20.00 $mmol{\cdot}L^{-1}$ et trois rapports molaires Ca/P (1,00, 1,50 et 2,00). Les pH initiaux (5,50, 6,70, 7,50, 8,50 et 9,50) étaient dérivants ou maintenus constants pendant un temps de réaction de 3 heures. Après filtration des suspensions, les compositions minérales des filtrats ont été analysées. Les précipités lyophilisés ont été caractérisés par diffraction des rayons X, spectroscopie infrarouge et microscopie électronique à balayage. À pH dérivant (pH final des suspensions compris entre 4,6 et 6,0), l'analyse minérale a montré que le rapport Ca/P n'influençait pas les quantités de phosphate et de calcium précipitées. Les analyses des précipités ont montré la formation de brushite comme principale phase cristalline. À pH constant, l'analyse minérale a montré que le rapport Ca/P avait une forte influence sur le taux de précipitation du phosphate de calcium. Les analyses des précipités ont mis en évidence la formation d'apatites déficientes en calcium mal cristallisées. Une diminution de la cristallinité avec l'augmentation du pH initial a été observée. En conclusion, le pH peut être considéré comme un facteur essentiel pour contrôler la quantité et la structure cristalline des phosphates de calcium obtenus par précipitation. Ce facteur est à considérer dans la récupération des phosphates de calcium des co-produits laitiers. Le pH est également important dans les phénomènes d'encrassement des membranes et des échangeurs thermiques suite à la précipitation du phosphate de calcium.

lait / produits laitiers / phosphate de calcium / précipitation / brushite

1. INTRODUCTION

The precipitation of calcium phosphate has been the subject of intensive research in different areas such as medicine (formation of kidney stones, (de)calcification of bone and tooth enamel and elaboration of materials for biomedical applications) [20, 23, 30] and environment (phosphorus removal from wastewater) [12, 32–34]. A number of studies reported in the literature showed that the formation of calcium phosphate is a complex phenomenon leading to the formation of different phases: brushite or dicalcium phosphate dehydrate (DCPD), octacalcium phosphate (OCP), hydroxyapatite (HAP) or calcium-deficient apatite (CDA) depending on the experimental conditions [5, 9, 11, 14, 17, 18]. The main conditions influencing the precipitation of calcium phosphate are temperature, phosphate and calcium concentrations, ionic strength, pH, the presence of other ions and the duration of precipitation [15, 16, 19]. The characteristics of calcium phosphate phases formed in different physico-chemical conditions and their chemical reactions are summarized in Table I.

Table I. Characteristics of calcium phosphate phases. K_{sp}, solubility product constant.

Solid phase	Chemical reaction in aqueous solutions	Ca/P	−Log K_{sp}	Formation conditions pH/temperature (°C)	References
Brushite or DCPD	$Ca^{2+} + HPO_4^{2-} + 2H_2O = CaHPO_4{\cdot}2H_2O$ (aq)	1	6.68	4–6/25; 4–6/37; 4/60	[11, 14, 17]
OCP	$8Ca^{2+} + 2HPO_4^{2-} + 4PO_4^{3-} + 5H_2O =$ $Ca_8(HPO_4)_2(PO_4)_4{\cdot}5H_2O$ (aq)	1.33	46.9	6.5/37; 5/60; 4/80	[14]
HAP	$10Ca^{2+} + 6PO_4^{3-} + 2OH^- =$ $Ca_{10}(PO_4)_6(OH)_2$ (aq)	1.67	57.74	7–9/60; 6–9/80	[14, 18]
CDA	$(10-x)Ca^{2+} + xHPO_4^{2-} + (6-x)PO_4^{3-} + (2-x)OH^- =$ $(10-x/6)Ca_{10-x}(HPO_4)_x(PO_4)_{6-x}(OH)_{2-x}$ (aq)	$(0 < x \leq 2)$	–	7.5–9/37	[14]

In dairy science and technology, this phenomenon is less studied. However, some studies have been conducted on the precipitation of calcium phosphate in the dairy conditions using model or real systems. Thus, Van Kemenade and De Bruyn [35] addressed the kinetic study of calcium phosphate precipitation from supersaturated solutions with respect to some milk conditions. They investigated the formation and growth of crystallized phases (DCPD, OCP and HAP) and amorphous calcium phosphate (ACP) in different conditions of pH, temperature and supersaturation. Combining the growth curves and the relaxation time analysis, they described the kinetics of precipitating systems and confirmed the validity of the Ostwald rule of stages [35]. In a similar context, Schmidt and Both [27] showed that DCPD is the first precipitating phase obtained when they mixed calcium and phosphate at 25 and 50 °C in the pH range 5.3–6.8 at an ionic strength of about 0.1. More recently, studies investigating the calcium phosphate precipitation, using model fluids (simulated milk ultrafiltrate solutions without proteins) were conducted [1, 25, 29]. These studies aimed to best understand the fouling of milk heat exchangers caused by calcium phosphate deposition at temperature 50–70 °C. Spanos et al. [29] observed a deposit formation of ACP at 60 and 70 °C in the pH range of 6–6.4. In similar conditions of temperature (55–75 °C) and pH (5.7–7.0), Andristos et al. [1] showed the precipitation of ACP followed by the formation of low crystallized prisms of HAP. The crystallinity was improved with the solution ageing. Using a real system (sweet whey permeate), Pouliot et al. [22] investigated the induction of ACP precipitation using a simple alkalinization or an alkalinization-seeding combination. The second technique induced an extensive crystallization of calcium phosphate. Saulnier et al. [26] showed the presence of brushite in various industrial wheys using X-ray diffraction (XRD) technique. Formation of calcium phosphate in relation with the mechanisms of membrane fouling was also studied. Thus, Rice et al. [24] observed that calcium phosphate was the predominant foulant leading to flux decline in nanofiltration of dairy ultrafiltration permeate, but the nature of the calcium phosphate was not determined. Labbe et al. [13] and Gesan et al. [7] indicated the presence of calcium phosphate at the membrane surface during crossflow microfiltration of preheated whey or during whey ultrafiltration.

In spite of these different studies, there is an imperative need of additional information about the effects of the controlling and influencing factors on the precipitation of calcium phosphates. For these reasons, in this study, we investigated the effects of Ca/P molar ratio and the pH values, left to drift or maintained constant, on the characteristics of calcium phosphate precipitates. Because of the richness of milk in various minerals, proteins and other organic components, which can interact among themselves, the understanding of this phenomenon is difficult. Hence, to facilitate the interpretation of the results, the precipitation of calcium phosphate was studied using simple solutions under controlled conditions. The quantitative study was carried out by monitoring the pH of precipitation and by determining the calcium and phosphate contents in precipitates. The structure of precipitates was evaluated using XRD, Fourier transform infrared spectroscopy (FTIR) and scanning electron microscopy (SEM) techniques. This research is of particular interest for the understanding of calcium phosphate formation under controlled physico-chemical conditions and for the recovery of calcium phosphates in dairy industry.

2. MATERIALS AND METHODS

2.1. Chemicals and reagents

Stock solutions of 1 $mol \cdot L^{-1}$ calcium chloride ($CaCl_2 \cdot 2H_2O$) (Sigma, Tokyo,

Japan) and 0.5 mol·L^{-1} sodium hydrogenophosphate at different pH values (5.50, 6.70, 7.50, 8.50 and 9.50) were prepared. These five phosphate solutions were made by neutralization of ortho-phosphoric acid solutions (Fluka BioChemika, Buchs, Switzerland) with 1 mol·L^{-1} NaOH solution (VWR, Fontenay-sous-Bois, France) until the desired pH values were reached. Milli-Q water was used in the different experiments.

2.2. Calcium phosphate precipitation

The precipitation experiments were performed by mixing the stock solutions of calcium chloride and sodium hydrogenophosphate. The initial solutions had a 20.00 mmol·L^{-1} phosphate concentration and 1.00, 1.50 and 2.00 Ca/P molar ratios. The initial pH (5.50, 6.70, 7.50, 8.50 and 9.50 ± 0.03) were drifting or maintained constant by the addition of NaOH 2 mol·L^{-1} using a pH-stat system (Metrohm, 702 SM Titrino model, Herisau, Switzerland). The precipitation experiments were conducted for 3 h by adding the relevant calcium concentrations diluted in 40–200 mL phosphate solutions contained in a jacketed glass cell of 240 mL final volume. The temperature was regulated by a water jacket and a thermostatic bath maintained at 20 ± 0.5 °C. Precipitation experiments were carried out under continuous stirring with a propeller stirrer operating at 400 rpm. Analysis of variance (ANOVA) was used to establish the statistical significance of the effects of initial pH and initial Ca/P molar ratio on the extents of pH drifting.

2.3. Solution filtration and precipitate lyophilization

The suspensions were filtered (Whatman 42 filter papers) without washing to avoid possible dissolution of part of the solid. The precipitates were lyophilized (RP2V, SGD Sérail, Argenteuil, France) and stored in sealed containers at room temperature before analyses.

2.4. Chemical and physical characterizations of precipitates

2.4.1. Calcium and phosphate contents

The calcium and phosphate contents were determined in the total sample and in the filtrates using atomic absorption spectrometry (Varian 220FS spectrometer, Les Ulis, France) and using ion chromatography (Dionex DX 500, Dionex, Voisin-le-Bretonneux, France) [6], respectively. The experimental errors were ± 5%. Insoluble calcium and phosphate concentrations were obtained by subtracting soluble concentrations that remained in filtrates from initial (total) calcium and phosphate concentrations, respectively.

2.4.2. Characterization of precipitates

The precipitates were analysed using XRD and FTIR techniques. The XRD patterns were recorded using a Philips PW 1830 X-ray generator equipped with a PW 1050 (θ/2θ) goniometer and a PW 1711 Xe detector. The data were acquired using Ni-filtered copper Kα radiation in a step-by-step mode with initial 2θ = 3°, final 2θ = 60°, step 2θ = 0.02° and time per step = 1.2 s. The FTIR spectra were obtained on a Nicolet Magnat II 550 FTIR spectrometer (400–4000 cm^{-1} spectral range with 4 cm^{-1} resolution and 32 cumulated scans), using the KBr pellet technique (1 mg of powder in 300 mg of KBr).

The morphology of the precipitates was observed using SEM technique (LEO 1450 VP, Carl Zeiss SMT, Oberkochen, Germany). Secondary electron images of samples were performed at an accelerated voltage of 5 kV. Before observation, samples were covered with a thin layer of gold-palladium deposited by sputtering evaporation.

3. RESULTS AND DISCUSSION

3.1. Effects of initial conditions on the pH decrease during calcium phosphate precipitation

The spontaneous precipitation of calcium phosphate from supersaturated solutions was accompanied by pH decrease. Figure 1 shows representative curves of pH evolution of the suspensions after mixing calcium and phosphate solutions. After calcium addition, the pH decreased quickly during the first few minutes, followed by an irregular and slow decrease during the next hour and finally became stable after 2 h.

The precipitation of calcium phosphate from supersaturated solutions is a complex phenomenon since several intermediate solid phases can precede the formation of the most thermodynamically stable phase [3]. For example, the formation of brushite from aqueous solutions occurred in five stages as described by Ferreira et al. [5]. In their model, the authors explained the decrease of pH observed in the beginning of the process by the HAP crystal growth preceding the appearance of the first nuclei of brushite. Andristos et al. [1] showed the precipitation of ACP followed by the formation of low crystallized prisms of HAP in the simulated milk ultrafiltrate solutions. The formation/dissolution of such intermediate phases may explain the irregularities in the pH changes observed in Figure 1.

To quantify the extent of pH decrease depending on the initial conditions, we calculated ΔpH corresponding to the absolute values of the difference between initial pH and terminal pH after 3 h. Figure 2 shows the relationship between ΔpH and the initial pH value for each mixture. ANOVA showed significant statistical effects of initial pH and Ca/P molar ratio on the ΔpH values ($P < 0.001$). In all samples, for the same initial pH, ΔpH increased with the initial Ca/P molar ratio and for the same initial Ca/P molar ratio, ΔpH increased with initial pH.

During the process of precipitation and crystal growth, the pH affects both the solution and the mineral surface [21]. In solution, the reduction of pH (ranged from 9.50 to 5.50 in the experiments) decreases the saturation state by shifting the equilibrium of phosphate species from PO_4^{3-} to HPO_4^{2-} to $H_2PO_4^-$ (equations (1) and (2)). The extent of pH decrease was higher at initial pH values of 7.50, 8.50 and 9.50. In this pH range, the predominant form of phosphate was HPO_4^{2-}. In the presence of sufficient concentration of calcium, and due to the relatively high affinity of HPO_4^{2-} to calcium (equation (3)), these ions interact to form a $CaHPO_4$ complex. When the precipitation of calcium phosphate occurred, the removal of HPO_4^{2-} ions from the $H_2PO_4^-/HPO_4^{2-}/PO_4^{3-}$ system shifts the equilibrium with the release of protons leading to the decrease of pH (equation (2)). At the mineral surface, the pH can shift the surface charge of the solid by changing the distribution of protons and hydroxyl groups hydrating the interface [10]. Equilibria in solution and at the interface (during the crystal growth) can explain the changes in pH during the precipitation of calcium phosphate from supersaturated solutions [5, 21].

$$PO_4^{3-} + H^+ \Longleftrightarrow HPO_4^{2-} \quad pK = 12.39 \quad (1)\ [28]$$

$$HPO_4^{2-} + H^+ \Longleftrightarrow H_2PO_4^- \quad pK = 7.05 \quad (2)\ [28]$$

$$Ca^{2+} + HPO_4^{2-} \Longleftrightarrow CaHPO_{4\ (aq)} \quad K_a = 642\ M^{-1} \quad (3)\ [28]$$

3.2. Effects of initial conditions on the quantity of precipitates

Formation of precipitates was observed in all mixtures (at drifting or constant pH) except in those at 5.50 initial pH. Considering the used concentrations of calcium and

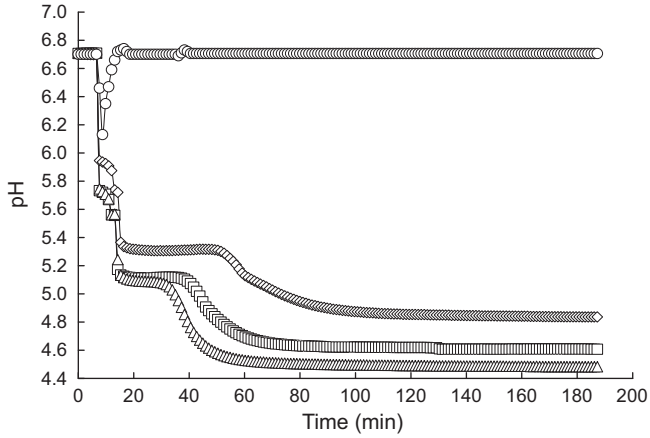

Figure 1. Representative recordings of the evolution of pH for 3 h after calcium addition to 20.00 mmol·L^{-1} phosphate at 6.70 constant (○) or drifting initial pH with 1.00 (◊), 1.50 (□) or 2.00 (Δ) initial Ca/P molar ratios. Measurements were carried out under continuous stirring using the pH-stat device.

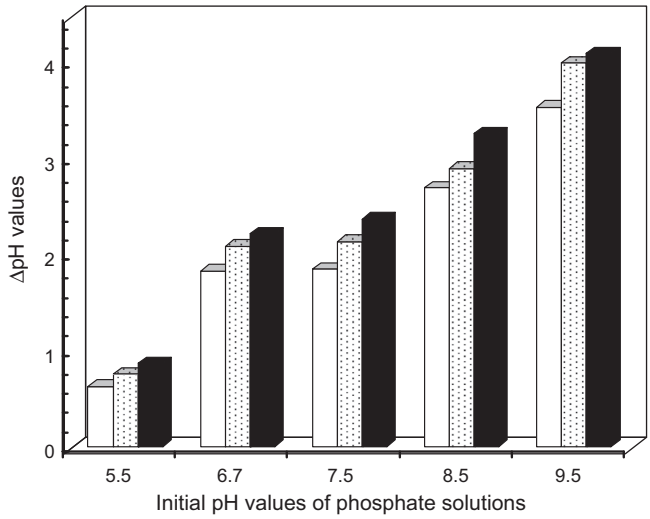

Figure 2. Relationship between ΔpH (the absolute value of the difference between initial and terminal pH) and the initial pH at 1.00 (▯), 1.50 (▤) or 2.00 (▮) Ca/P initial molar ratios.

phosphate, the temperature (20 °C) and the reaction time (3 h) in the experiments, the solubility isotherms of different calcium phosphates showed that the supersaturation (with respect to brushite) was not reached at pH 5.50 [36]. This explains the absence of precipitate at pH 5.50 and the low quantity of precipitate at pH 6.70

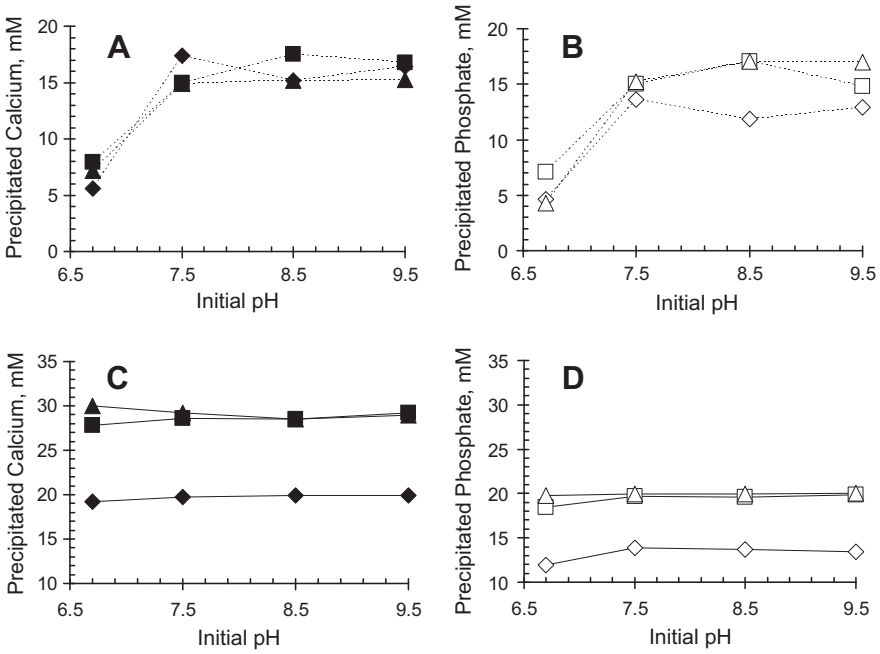

Figure 3. Amounts of precipitated calcium (black) and phosphate (white) obtained with 1.00 (◊), 1.50 (□) or 2.00 (Δ) Ca/P molar ratios at drifting (A and B) or constant (C and D) initial pH values.

in comparison with those obtained at 7.50, 8.50 and 9.50 initial pH (Fig. 3).

Figures 3A and 3B show the amounts of precipitated calcium and phosphate at drifting pH (initial values were 6.70, 7.50, 8.50 and 9.50). Amounts of precipitated calcium and phosphate increased from about 7 ± 1.5 mmol·L^{-1} to about 16 ± 1 mmol·L^{-1} between 6.70 and 7.50 initial pH and tend to stabilize between 7.50 and 9.50 initial pH. This trend was observed whatever the initial Ca/P molar ratio was. These results indicated that the quantities of precipitated calcium phosphate obtained at drifting pH are mainly influenced by the pH of precipitation. After a reaction time of about 1 h, the final pH of the solutions became stable with values ranged from 4.48 to 5.96 (Tab. II). At these pH values, the supersaturation state of calcium phosphates is reduced. This can explain the low precipitation efficiency of phosphate which was about 60–85% for experiments at 7.50, 8.50 and 9.50 initial pH and only about 21–35% at 6.70 initial pH (Tab. II).

Figures 3C and 3D show the amounts of precipitated calcium and phosphate at constant pH. The amounts of precipitated calcium and phosphate at constant pH were mainly modulated by the Ca/P molar ratio in the precipitates estimated to about 1.48. Indeed, precipitated calcium and phosphate amounts (on average 29 and 19.5 mmol·L^{-1}, respectively) were similar in case of 1.50 and 2.00 initial Ca/P ratios but are much lower in case of 1.00 initial Ca/P molar ratio (on average 19.5 mmol·L^{-1} calcium and 14 mmol·L^{-1} phosphate). Considering the rates of calcium and phosphate precipitation expressed in percentage of the total

Table II. Characteristics of the suspensions and precipitates of calcium phosphates obtained at drifting pH (* traces of OCP). Precipitate analyses performed using XRD and FTIR.

Initial conditions		Terminal conditions							Precipitate characterization		
pH	Ca/P	pH	ΔpH	Precipitated calcium		Precipitated phosphate		Ca/P	XRD		FTIR
				$mmol \cdot L^{-1}$	% total	$mmol \cdot L^{-1}$	% total				
6.70	1.00	4.84	1.86	5.60	28.00	5.33	26.65	1.05	Brushite		Brushite
6.70	1.50	4.61	2.09	7.90	26.33	7.07	35.35	1.12	Brushite		Brushite
6.70	2.00	4.48	2.22	7.17	17.93	4.28	21.40	1.67	Brushite		Brushite
7.50	1.00	5.75	1.75	17.40	87.00	13.63	68.15	1.28	Brushite		Brushite
7.50	1.50	5.36	2.14	14.96	49.87	14.99	74.95	1.00	Brushite		Brushite
7.50	2.00	5.13	2.37	14.91	37.28	15.26	76.30	0.98	Brushite		Brushite
8.50	1.00	5.83	2.67	15.20	76.00	11.87	59.35	1.28	Brushite		Brushite
8.50	1.50	5.6	2.90	17.53	58.43	17.03	85.15	1.03	Brushite		Brushite
8.50	2.00	5.37	3.13	15.15	37.88	17.06	85.30	0.89	Brushite		Brushite
9.50	1.00	5.96	3.54	16.40	82.00	12.93	64.65	1.27	Brushite	OCP*	Brushite
9.50	1.50	5.5	4.00	16.73	55.77	14.82	74.10	1.13	Brushite	OCP*	Brushite
9.50	2.00	5.4	4.10	15.24	38.10	16.97	84.85	0.90	Brushite	OCP*	Brushite

Table III. Characteristics of the suspensions and precipitates of calcium phosphates obtained at constant pH. Precipitate analyses performed using XRD and FTIR. CDA. (Crystalline * ** *** amorphous).

Initial conditions		Terminal conditions						Precipitate characterization	
pH	Ca/P	pH	Precipitated calcium		Precipitated phosphate		Ca/P	XRD	FTIR
			$mmol \cdot L^{-1}$	% total	$mmol \cdot L^{-1}$	% total			
6.70	1.00	6.70	19.18	95.90	11.93	59.65	1.61	CDA*	CDA
6.70	1.50	6.70	27.81	92.70	18.43	92.15	1.51	CDA*	CDA
6.70	2.00	6.70	29.96	74.90	19.78	98.90	1.51	CDA*	CDA
7.50	1.00	7.50	19.76	98.80	13.89	69.45	1.42	CDA*	CDA
7.50	1.50	7.50	28.60	95.33	19.68	98.40	1.45	CDA*	CDA
7.50	2.00	7.50	29.20	73.00	19.95	99.75	1.46	CDA*	CDA
8.50	1.00	8.50	19.94	99.70	13.69	68.45	1.46	CDA**	CDA
8.50	1.50	8.50	28.50	95.00	19.64	98.20	1.45	CDA**	CDA
8.50	2.00	8.50	28.54	71.35	19.95	99.75	1.43	CDA**	CDA
9.50	1.00	9.50	19.92	99.96	13.47	67.35	1.48	CDA***	CDA
9.50	1.50	9.50	29.22	97.40	19.85	99.25	1.47	CDA***	CDA
9.50	2.00	9.50	28.96	72.40	19.99	99.95	1.45	CDA***	CDA

(Tab. III), the initial Ca/P ratio of 1.50 gave the highest precipitation efficiency. When initial Ca/P was 1.00, calcium concentration was the limiting factor and when initial Ca/P was 2.00, phosphate concentration was the limiting one. Whatever be the initial

Ca/P molar ratio, the phosphate precipitation efficiency is higher at constant pH than at drifting pH.

Finally, the Ca/P molar ratios in the precipitates obtained at different initial conditions are shown in Tables II and III. The final Ca/P ratio can give some indication on the precipitating phase but cannot provide the exact crystalline structure of the precipitates particularly when several solid phases or ACP are formed. The Ca/P molar ratios in the precipitates at drifting pH were on average equal to 1.00 (Tab. II), close to that of brushite. These results agree with those of Schmidt and Both [27] obtained at 25 °C and at pH values < 6.84. The Ca/P ratios in the precipitates at constant pH were about 1.48 (Tab. III), close to that of tricalcium phosphate (1.50) or non-stoichiometric apatites. As the presence of tricalcium phosphate was unlikely in our experiment conditions because its formation requires very high temperature (800–1200 °C), the precipitating solid should be an apatitic type [3, 4, 14].

3.3. Identification of the solid phases in precipitates

Three complementary techniques were used for precipitate characterization. The XRD analysis gives information on the crystal structure and atomic arrangements of materials, whereas the FTIR technique provides information on the chemical composition and vibrational modes enabling detection of both crystalline and amorphous phases. Observations with SEM technique show the morphology (size, shape and crystallinity) of particles.

These techniques are used for the characterization of the final solid. The crystallization of calcium phosphates from aqueous solutions requires a sufficient supersaturation and involves many steps, namely nucleation, crystal growth and aggregation [8]. The precipitation process is a complex phenomenon since different phases can be obtained, depending on the experimental conditions [1, 5]. Johnsson and Nancollas [11] reported that precipitation reactions at sufficiently high supersaturation and pH result in the initial formation of ACP, which is a highly unstable phase. The primary nuclei of ACP hydrolyze almost instantaneously to more stable phases. The reaction time (or ageing) is an important factor influencing the crystallinity of the precipitating phase. In this study, the precipitates characterized as described hereafter were obtained exactly after 3 h of precipitation at drifting or constant pH. The different phases of calcium phosphate that will be addressed hereafter are summarized in Table I.

3.3.1. XRD technique

Figure 4A shows XRD patterns of calcium phosphate precipitates obtained at drifting pH (initial pH of 6.70, 7.50, 8.50 and 9.50) with 1.50 initial Ca/P molar ratio. All precipitates obtained at drifting pH with 1.00, 1.50 or 2.00 initial Ca/P molar ratios (results not shown) had very similar XRD pattern profiles. The high-intensity peaks (at 2θ angles of 11.66, 20.96, 29.33, 30.56 and 34.19°) correspond to the characteristic pattern of brushite, $CaHPO_4{\cdot}2H_2O$ (ICDD file 00-009-0077). These results confirm the formation of brushite as the main crystalline structure in the precipitates at drifting pH. Indeed, terminal pH values of the suspensions were ranged 4.48–5.96 (Tab. II) promoting the formation of brushite [5, 16]. These results agree with those obtained by Schmidt and Both [27] in a model system and also with those of Calco [2] and Saulnier et al. [26]. These authors reported the presence of brushite in industrial wheys with pH values that ranged from 4.60 to 6.20. We note that samples obtained at drifting 8.50 and 9.50 initial pH (Fig. 4A) have XRD patterns less resolved indicating a possible presence of other phases in addition to brushite. Indeed, the low-intensity peak at around 2θ angles = 4.73° in sample at 9.50 drifting pH indicated the possible presence

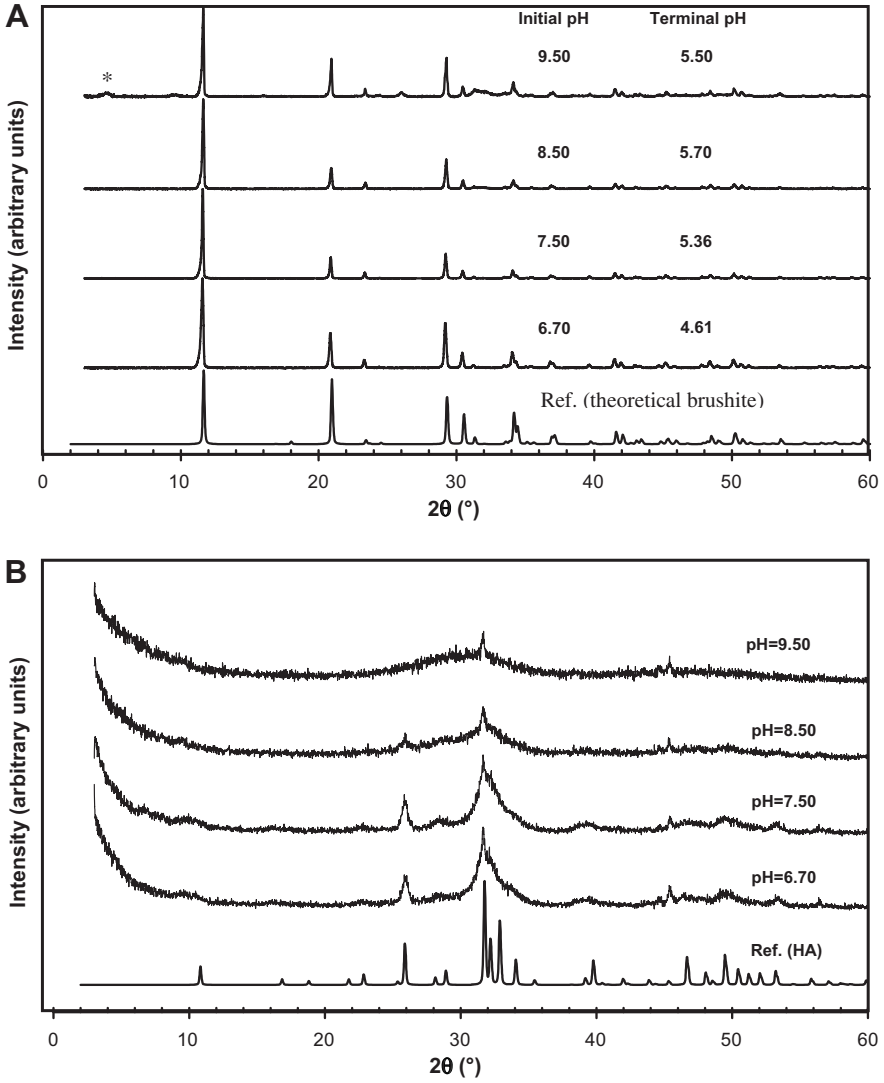

Figure 4. XRD patterns of calcium phosphate precipitates obtained at different drifting (A) or constant (B) initial pH values (6.70, 7.50, 8.50 and 9.50) from solutions at 20.00 mmol·L^{-1} phosphate concentration and 1.50 Ca/P molar ratio. The spectra are compared to diffraction patterns of HAP and brushite simulated from their respective crystal structures (ICSD files codes 22060 and 16132, respectively). Asterisk denotes possible traces of OCP.

of OCP. Schmidt and Both [27] reported the crystallization of OCP and DCPD in solution at acidic pH (5.3–6.84), but the formation of OCP occurred mainly at 50 °C. In comparison to standard pattern of brushite, variation in the peak intensity ratio between the two peaks at 2θ angles of 11.66 and 20.96° was observed (Fig. 4A)

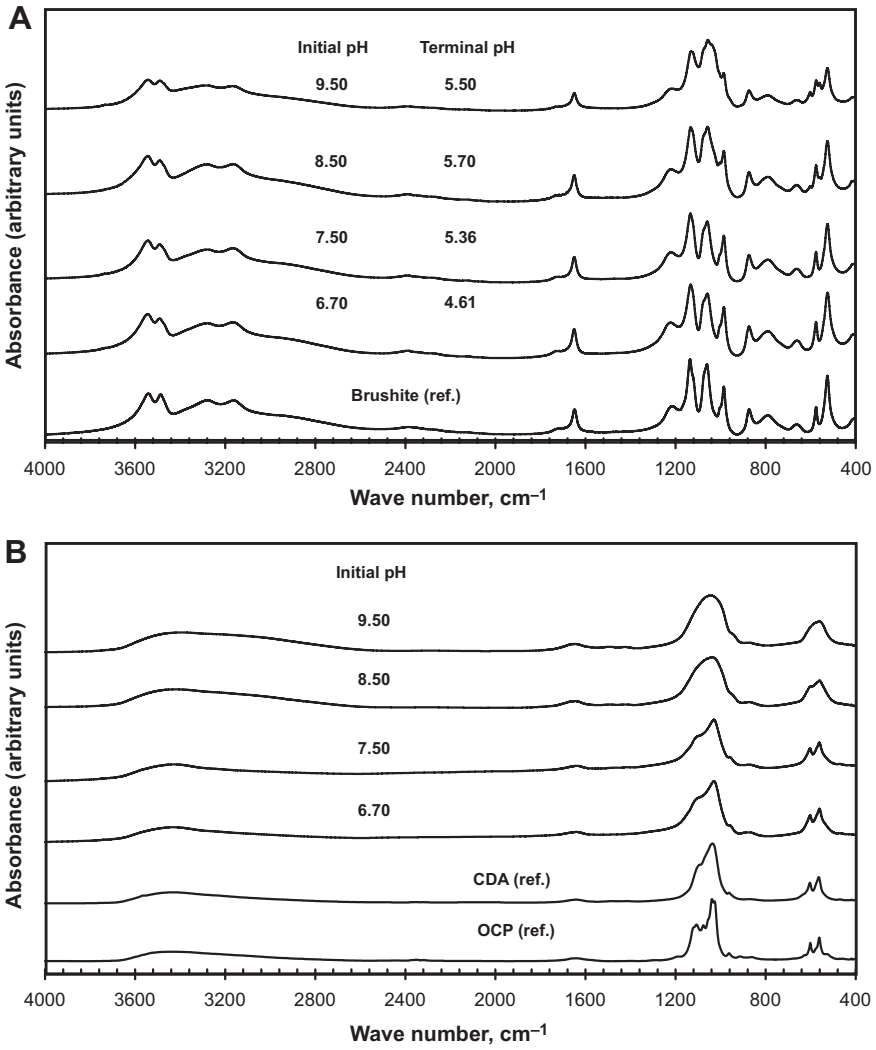

Figure 5. The FTIR spectra of calcium phosphate precipitates obtained at drifting (A) or constant (B) initial pH values (6.70, 7.50, 8.50 and 9.50) from solutions at 20.00 mmol·L^{-1} initial phosphate concentration and 1.50 Ca/P molar ratio. They are compared to standard spectra of brushite, CDA and OCP.

suggesting preferential orientation of crystallites. Yet, when preparing samples for XRD analyses, powders were finely crushed in an agate mortar using a pestle in order to avoid, as much as possible, the preferential orientation of crystallites.

Figure 4B shows XRD patterns of standard HAP and calcium phosphate precipitates obtained at constant pH (6.70, 7.50, 8.50 and 9.50) with 1.50 initial Ca/P molar ratio. These results were similar to those of precipitates obtained with 1.00 and

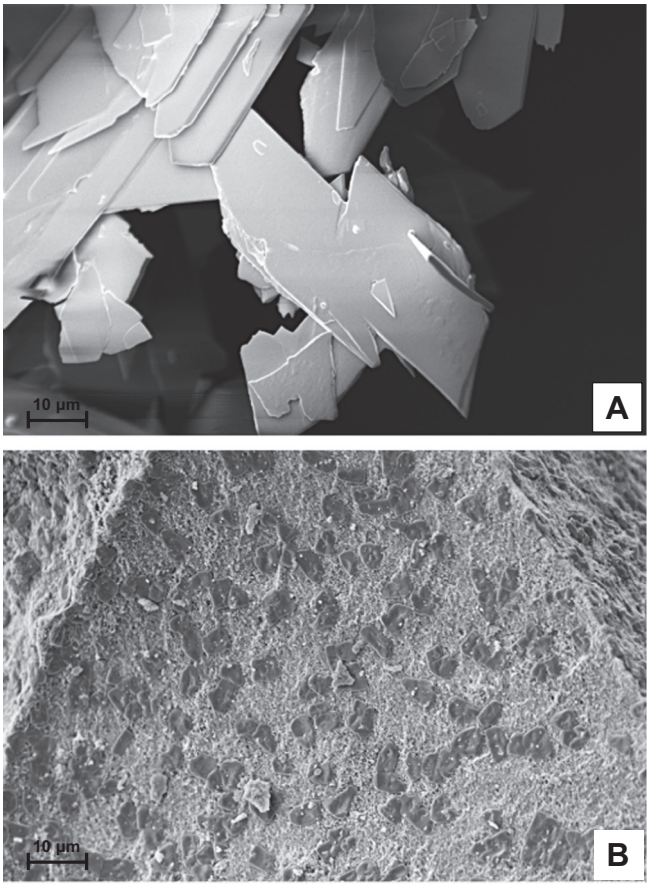

Figure 6. Representative SEM images of calcium phosphate precipitates obtained from solutions at 20.00 mmol·L^{-1} phosphate and 1.50 Ca/P molar ratio at drifting (A) or constant (B) 6.70 initial pH.

2.00 initial Ca/P ratios (results not shown). In comparison with XRD patterns of precipitates obtained at drifting pH (Fig. 4A), crystalline brushite was not found. Raw recorded patterns showed an increase in noisy signal as the pH values increased indicating a low crystallinity in these samples. Nevertheless, at least three diffraction maxima (at 2θ angles of 25.91, 31.76 and 49.49°) with strong intensity were observed. They were coincident with some of the most important maxima of HAP. These results suggest the formation of CDA as the main low crystallized phase in precipitates obtained at neutral or moderately alkaline solutions (Tab. III and Fig. 4B). All these results confirm the dominant effect of pH factor on the crystallization of calcium phosphates in aqueous solutions with different chemical composition. Considering the solubility products of calcium phosphate phases, the supersaturation required for their precipitation is in the order HAP > OCP > DCPD [31]. In spite of this fact, DCPD nucleates more easily than OCP and HAP at low pH, while OCP nucleates more easily than HAP at mean

to high pH. Our results are in agreement with these observations. Thus, at 20 °C, the formation of brushite is promoted at acidic pH and that of CDA at higher pH.

3.3.2. FTIR technique

Figure 5 shows FTIR spectra of calcium phosphate precipitates obtained at drifting (A) and constant (B) initial pH (6.70, 7.50, 8.50 and 9.50) from solutions with 1.50 initial Ca/P molar ratio. The FTIR spectra of all precipitates had very similar profiles whatever be the initial Ca/P molar ratio (results not shown).

At drifting pH (Fig. 5A), all bands were assigned to phosphate groups that are characteristic of brushite. However, the low resolution of some bands (400–1200 cm^{-1}) at 9.50 drifting pH indicates a low crystallinity or a possible presence of another calcium phosphate phase.

At constant pH (Fig. 5B), FTIR spectra show broadly similar profiles with low resolution. In order to identify the samples, spectra were compared to characteristic fingerprints of OCP and CDA. The absence of bands located around 1076 cm^{-1} corresponding to P-O antisymmetric stretching (ν_3 PO_4^{3-} and HPO_4^{2-}) characteristic of OCP confirms that CDA was the main phase formed at constant pH values. On the other hand, the bands between 565 and 610 cm^{-1} become less resolved at high initial pH values (8.50 and 9.50). This indicated a very low crystallinity of the precipitating solid which can involve amorphous forms of calcium phosphates whose precipitation is favoured at alkaline pH. It is reported that the conversion of ACP to more crystallized calcium phosphates may occur after several weeks [3, 14].

3.3.3. SEM technique

Observations by SEM technique (Figs. 6A and 6B) showed the morphology and crystallinity state of the precipitates. At drifting pH, SEM technique revealed the formation of typical plate-like brushite crystals (Fig. 6A). In precipitates obtained at constant pH, Figure 6B shows that the formed phase has a very low crystallinity state that eventually would convert into a more crystallized apatite phase over a period of time. These observations confirmed the results obtained with XRD and FTIR techniques.

4. CONCLUSION

In this study, we investigated the effects of drifting or constant initial pH and the initial Ca/P molar ratio on the precipitation of calcium phosphate from aqueous solution. Our results showed that, at drifting initial pH, the Ca/P molar ratio did not influence the amounts of precipitated calcium and phosphate. The precipitation efficiency of calcium phosphate increased when pH was kept constant in comparison with precipitation at drifting pH. Considering the initial Ca/P molar ratio, we can conclude that 1.50 gave the highest precipitation efficiency, whereas when initial Ca/P was 1.00, calcium concentration was the limiting factor and when initial Ca/P was 2.00, phosphate concentration was the limiting one. The XRD, FTIR and SEM analyses showed that pH was the main factor influencing the crystalline structure of calcium phosphate precipitates. When initial pH was left to drift after calcium addition, brushite was found in all precipitates as the main crystalline phase. When initial pH was maintained constant, no brushite was found in precipitates but the presence of low crystallized CDA was determined. CDA crystallinity decreased with increasing initial pH. This research is of particular interest for the understanding of calcium phosphate formation (quantity and crystalline structure) under controlled physico-chemical conditions. The pH should be considered for the recovery of calcium phosphates from dairy

co-products. This factor is also important in the fouling phenomena of membranes and heat exchangers caused by calcium phosphate precipitation.

Acknowledgement: The authors thank Arilait Recherches, CNIEL (French Dairy Industry Association) for its financial support and valuable advice and discussions.

REFERENCES

[1] Andritsos N., Yiantsios S.G., Karabelas A.J., Calcium phosphate scale formation from simulated milk ultrafiltrate solutions, Food Bioprod. Process. 80 (2002) 223–230.

[2] Calco M., Valorization of industrial wheys using membrane processes, Ph.D. Thesis, Université de Nancy 1, Nancy, France, 1997.

[3] Elliott J.C., Structure and chemistry of the apatite and other calcium orthophosphates, Elsevier Science B.V., Amsterdam, 1994.

[4] Famery R., Richard N., Boch P., Preparation of α- and β-tricalcium phosphate ceramics, with and without magnesium addition, Ceram. Int. 20 (1994) 327–336.

[5] Ferreira A., Oliveira C., Rocha F., The different phases in the precipitation of dicalcium phosphate dehydrate, J. Cryst. Growth 252 (2003) 599–611.

[6] Gaucheron F., Le Gräet Y., Piot M., Boyaval E., Determination of anions of milk by ion chromatography, Lait 76 (1996) 433–443.

[7] Gesan G., Daufin G., Merin U., Labbé J.P., Quémerais A., Fouling during constant flux crossflow microfiltration of pretreated whey, Influence of transmembrane pressure gradient, J. Membr. Sci. 80 (1993) 131–145.

[8] Giulietti M., Seckler M.M., Derenzo S., Re M.I., Cekinski E., Industrial crystallization and precipitation from solutions: state of the technique, Braz. J. Chem. Eng. 18 (2001) 423–440.

[9] Guo L.F., Wang W.H., Zjang W.G., Wang C.T., Effects of synthesis factors on the morphology, crystallinity and crystal size of hydroxyapatite precipitation, J. Harbin Inst. Technol. 12 (2005) 656–660.

[10] Harding I.S., Rashid N., Hing K.A., Surface charge and the effect of excess calcium ions on the hydroxyapatite surface, Biomaterials 26 (2005) 6818–6826.

[11] Johnsson M.S.A., Nancollas G.H., The role of brushite and octacalcium phosphate in apatite formation, Crit. Rev. Oral Biol. Med. 3 (1992) 61–82.

[12] Joko I., Phosphorus removal from wastewater by the crystallization method, Water Sci. Technol. 17 (1984) 121–132.

[13] Labbe J.P., Quemerais A., Michel F., Daufin G., Fouling of inorganic membranes during whey ultrafiltration: analytical methodology, J. Membr. Sci. 165 (1990) 293–307.

[14] LeGeros R.Z., Calcium phosphates in oral biology and medicine, New York University College of Dentistry, New York, 1991.

[15] Madsen H.E.L., Christensson F., Precipitation of calcium phosphate at 40 °C from neutral solution, J. Cryst. Growth 114 (1991) 613–618.

[16] Madsen H.E.L., Thorvardarson G., Precipitation of calcium phosphate from moderately acid solution, J. Cryst. Growth 66 (1984) 369–376.

[17] Marshall R.W., Nancollas G.H., The kinetics of crystal growth of dicalcium phosphate dehydrate, J. Phys. Chem. 73 (1969) 3838–3844.

[18] Mc Dowell H., Gregory T.M., Brown W.E., Solubility of $Ca_5(PO_4)_3OH$ in the system $Ca(OH)_2$-H_3PO_4-H_2O at 5, 15, 25, and 37 °C, J. Res. Nat. Bur. Stand. 81 (1977) 273–281.

[19] Nancollas G.H., Physical chemistry of crystal nucleation, growth and dissolution of stones, in: Wickham J.E.A., Buck A.C. (Eds.), Renal Tract Stone, Metabolic Basis and Clinical Practice, Churchill Livingstone, Edinburgh, 1990, pp. 71–85.

[20] Nancollas G.H., Lore M., Perez L., Richardson C., Zawacki S.J., Mineral phases of calcium phosphate, Anat. Rec. 224 (1989) 234–241.

[21] Orme C., Giocondi J., Model systems for formation and dissolution of calcium phosphate minerals, in: Behrens P., Baeuerlein E. (Eds.), Handbook of Biomineralization: Biomimetic and Bio-inspired Materials Chemistry, Wiley-VCH, Weinheim, 2007, pp. 135–157.

[22] Pouliot Y., Landry J., Giasson J., Induction of calcium phosphate precipitation in sweet whey permeate, Lait 71 (1991) 313–320.

[23] Raynaud S., Champion E., Bernache-Assollant D., Thomas P., Calcium phosphate apatites with variable Ca/P atomic ratio. I. Synthesis, characterisation and thermal stability of powders, Biomaterials 23 (2002) 1065–1072.

[24] Rice G., Kentish S., O'Connor A., Stevens G., Lawrence N., Barber A., Fouling behaviour during the nanofiltration of dairy ultrafiltration permeate, Desalination 199 (2006) 239–241.

[25] Rosmaninho R., Rizzo G., Muller-Steinhagen H., Melo L.F., Deposition from a milk mineral solution on novel heat transfer surfaces under turbulent flow conditions, J. Food Eng. 85 (2008) 29–41.

[26] Saulnier F., Ferrero F., Bottero J.Y., Linden G., Variation of the composition and nature of the insoluble precipitate from industrial wheys, Lait 75 (1995) 93–100.

[27] Schmidt D.G., Both P., Studies on the precipitation of calcium phosphate. I. Experiments in the pH range 5.3 to 6.8 at 25 °C and 50 °C in the absence of additives, Neth. Milk Dairy J. 41 (1987) 105–119.

[28] Smith R.M., Mattell A.E., Critical stability constants, Vols. 1–6, Plenum Press, New York, 1976.

[29] Spanos N., Patis A., Kanellopoulou D., Andritsos N., Koutsoukos P.G., Precipitation of calcium phosphate from simulated milk ultrafiltrate solutions, Cryst. Growth Des. 7 (2007) 25–29.

[30] Suvorova E.I., Buffat P.A., Electron diffraction and high resolution transmission electron microscopy in the characterization of calcium phosphate precipitation from aqueous solutions under biomineralization conditions, Eur. Cell. Mater. 1 (2001) 27–42.

[31] Tung M.S., Calcium phosphates: structure, composition, solubility, and stability, in: Amjad Z. (Ed.), Calcium phosphates in biological and industrial systems, Kluwer Academic Publishers, Norwell, Massachusetts, 1998, pp. 1–19.

[32] Valsami-Jones E., Mineralogical controls on phosphorus recovery from wastewaters, Mineral. Mag. 65 (2001) 611–620.

[33] Van der Houwen J.A.M., Cressey G., Cressey B.A., Valsami-Jones E., The effect of organic ligands on the crystallinity of calcium phosphate, J. Cryst. Growth 249 (2003) 572–583.

[34] Van der Houwen J.A.M., Valsami-Jones E., The application of calcium phosphate precipitation chemistry to phosphorus recovery: the influence of organic ligands, Environ. Technol. 22 (2001) 1325–1335.

[35] Van Kemenade M.J.J.M., De Bruyn P.L., A kinetic study of precipitation from supersaturated calcium-phosphate solutions, J. Col. Interface Sci. 118 (1987) 564–585.

[36] Vereecke G., Lemaitre J., Calculation of the solubility diagrams in the system $Ca(OH)_2$-H_3PO_4-KOH-HNO_3-CO_2-H_2O, J. Cryst. Growth 104 (1990) 820–832.